JTTEE5 25:282–290
DOI: 10.1007/s11666-015-0311-6
1059-9630/$19.00 © ASM International

Peer Reviewed

Thermal Gradient Behavior of TBCs Subjected to a Laser Gradient Test Rig: Simulating an Air-to-Air Combat Flight

Rogerio S. Lima, Basil R. Marple, and P. Marcoux

(Submitted May 8, 2015; in revised form July 27, 2015)

A computer-controlled laser test rig (using a CO_2 laser) offers an interesting alternative to traditional flame-based thermal gradient rigs in evaluating thermal barrier coatings (TBCs). The temperature gradient between the top and back surfaces of a TBC system can be controlled based on the laser power and a forced air back-face cooling system, enabling the temperature history of complete aircraft missions to be simulated. An air plasma spray-deposited TBC was tested and, based on experimental data available in the literature, the temperature gradients across the TBC system (ZrO_2-Y_2O_3 YSZ top coat/CoNiCrAlY bond coat/Inconel 625 substrate) and their respective frequencies during air-to-air combat missions of fighter jets were replicated. The missions included (i) idle/taxi on the runway, (ii) take-off and climbing, (iii) cruise trajectory to rendezvous zone, (iv) air-to-air combat maneuvering, (v) cruise trajectory back to runway, and (vi) idle/taxi after landing. The results show that the TBC thermal gradient experimental data in turbine engines can be replicated in the laser gradient rig, leading to an important tool to better engineer TBCs.

Keywords air plasma spray (APS), simulated fighter jet mission, thermal barrier coating (TBC), thermal cycling, thermal gradient laser test rig, YSZ

1. Introduction

1.1 Thermal Barrier Coatings (TBCs)

Thermal barrier coatings (TBCs) engineered via thermal spray processing are applied on the static metallic parts of the hot zones of gas turbines for aerospace applications. TBCs are employed to allow turbine engines to operate at higher temperatures, thereby, improving their performance. TBCs also improve the durability and lifetime of these superalloy components, by reducing their overall temperature and protecting them against the harsh environment of the turbine engines. Peak combustion temperatures up to 1500 °C and pressures up to 40 atmospheres can be reached around the combustion chamber region; therefore, these temperature levels exceed the melting point of the metallic parts (typically below 1400 °C). The thermally sprayed TBC-protected parts include the combustion chambers, vanes, transition ducts, thrust reversers, and afterburners (Ref 1, 2).

A thermally sprayed TBC system generally consists of a two-layered architecture (deposited on a Ni-based superalloy component), i.e., a ceramic top coat (e.g., ZrO_2-8 wt.%Y_2O_3, a.k.a., YSZ) and a superalloy metallic MCrAlY bond coat (BC) (M = Ni, Co, CoNi, or NiCo). In thermally sprayed TBCs for aerospace applications, the typical BC and YSZ top coat thickness ranges are 125-250 and 250-500 μm, respectively (Ref 2).

The main function of the MCrAlY BC is to increase the high temperature oxidation and corrosion resistance of the underlying superalloy (Ref 2). In addition, it also increases the bonding of the YSZ top coat on the component and serves as a buffer layer to mitigate residual stresses (e.g., coating deposition + coating aging effects at high temperature) and differences in the coefficient of thermal expansion (CTE) between the metallic superalloy substrate and the YSZ ceramic top coat (Ref 3). Due to its low thermal conductivity values (~1 W/mK) and high melting point (~2700 °C), the main function of the YSZ top coat is to provide a thermal insulating layer to avoid having the superalloy metallic components reach their softening or melting temperature levels (Ref 1, 2).

1.2 Thermal Spraying TBCs

The air plasma spray (APS) technique is the standard thermal spray deposition system for the YSZ top coat (static parts of the turbine engine), whereas different types of systems can be employed to deposit the MCrAlY BC. These standard BC deposition systems include APS itself, as well as high velocity oxygen-fuel (HVOF) and low-

This article is an invited paper selected from presentations at the 2015 International Thermal Spray Conference, held on May 11 to May 14, 2015, in Long Beach, CA, USA, and has been expanded from the original presentation.

Rogerio S. Lima and **Basil R. Marple**, National Research Council of Canada, 75 de Mortagne Blvd., Boucherville, QC J4B 6Y4, Canada; and **P. Marcoux**, Vac Aero International, 1365 Newton Street, Boucherville, QC J4B 5H2, Canada. Contact e-mail: rogerio.lima@cnrc-nrc.gc.ca.

pressure plasma spray (LPPS) techniques, a.k.a., vacuum plasma spray (VPS).

1.3 Flame-Based Thermal Gradient Rigs

Flame-based thermal gradient rigs replicate the thermal gradient (ΔT) between the YSZ top coat and the substrate back side by using a flame (e.g., natural gas and O_2) to heat the YSZ top coat and by cooling the substrate back side with a compressed air jet. Pyrometers are used to monitor the temperatures at the front and back sides of the samples. By using this approach, the desired temperature gradient across the TBC system can be achieved and different types of cycles can be set up (Ref 4). The typical substrate samples for this type of test are puck-shaped, exhibiting diameters of 2.5-3.0 cm and thicknesses of 3-6 mm. This is a well-regarded testing system by the turbine community.

1.4 Laser-Based Thermal Gradient Rigs

Laser-based thermal gradient rigs can also be employed to replicate the thermal gradient (ΔT) between the YSZ top coat and the substrate back side (Ref 5). In this case, a 3 kW CO_2 laser can be employed to generate the heat flux on the YSZ top coat and a compressed air jet cools the back surface of the substrate. By controlling the laser power and the intensity of the substrate back cooling, different ΔTs can be achieved. Pyrometers are used to monitor the temperatures at the front and back sides of the samples. The 3 kW CO_2 laser is the choice for materials like YSZ because it can yield a continuous beam exhibiting a wavelength of 10.6 μm. The YSZ, specifically, is non-transparent to wavelengths from 6 to 20 μm, i.e., it absorbs the laser radiation within this wavelength range, as shown by Manara et al. (Ref 6). The typical substrate samples for this type of test are puck-shaped, exhibiting diameters of ~2.5 cm and thicknesses of ~3 mm.

1.5 Simulating Service Conditions of Turbine Engines

The service conditions of turbine engines are typically treated as confidential information by the original engine manufacturers (OEMs) and aircraft end-users (e.g., the military). Little information is available in the open literature. Nonetheless, Mom and Hersbach (Ref 7) published a paper on the performance of coatings on the F100 first-stage turbine blades under simulated services conditions. The F100 is a Pratt and Whitney turbine employed in fighter jets, like the F-15 Eagle and F-16 Fighting Falcon. This was a joint study of the National Aerospace Laboratory (NRL) of Holland and the Dutch Air Force. A burner rig was employed to simulate 300 h using flight-by-flight test procedure, i.e., different missions involved different types of temperature profiles and their frequencies. Four mission types were defined: (i) air combat aero, (ii) air to ground, (iii) combat profile, and (iv) general flying. The blade substrate material in that study (Ref 7) was the directionally solidified Mar-M200+Hf and the coatings were aluminide and NiCoCrAlY. The exact service temperature (~1425 °C) could not be achieved because of the maximum gas temperature (1070 °C). Consequently, the blades were not air cooled. Nevertheless, the real metal temperatures were achieved (military (MIL) 1050 °C, cruise 813 °C, and idle 590 °C) (Ref 7).

For the blades in the earlier study, their relative temperature profiles and relative frequencies were plotted in graphs versus the mission time (Ref 7). The air combat aero profile mission, as shown in Fig. 1, was chosen to be simulated in the thermal gradient laser rig of the National Research Council of Canada (NRC, Boucherville, QC, Canada).

In addition to the flight simulation profile mission provided by Mom & Hersbach (Ref 7), the flight profile mission designed for this work was complemented with some additional information published in public sites available on the internet about the performance of turbines and fighter jet flight path characteristics in air-to-air combat missions, e.g., (Ref 8).

2. Experimental Procedure

2.1 Thermal Spraying

The substrate material employed in this study was the Ni-based superalloy Inconel 625. For aerospace applications in turbine engines, this material is used to engineer the combustion chambers, transition ducts, thrust reversers, and afterburners. The substrates exhibited a puck shape (2.5 cm (1″) diameter and 3.2 mm (1/8″) thick). Prior to thermal spraying, the substrates were degreased with acetone and grit-blasted (both sides) with white alumina (Al_2O_3) grit #60 (average size ~254 μm) at 60 psi (414 kPa). The roughness (R_a) value was 2.5 ± 0.2 μm ($n = 10$). The CoNiCrAlY BC (Amdry 995C, Oerlikon Metco, Westbury, NY, USA) and the YSZ top coat (Metco 204B-NS, Oerlikon Metco, Westbury, NY, USA) were the feedstock powders employed in this study for TBC production. The overall particle size range (in volume) for the CoNiCrAlY powder was d_{10}: 48 μm; d_{50}: 61 μm; and d_{90}: 79 μm, whereas that of the YSZ powder was d_{10}: 46 μm; d_{50}: 61 μm; and d_{90}: 80 μm. These values were determined via laser-scattering particle size analysis.

Both powders were deposited using an APS torch (Metco 3MB, Oerlikon Metco, Westbury, NY, USA). The complete set of spray parameters is considered as an

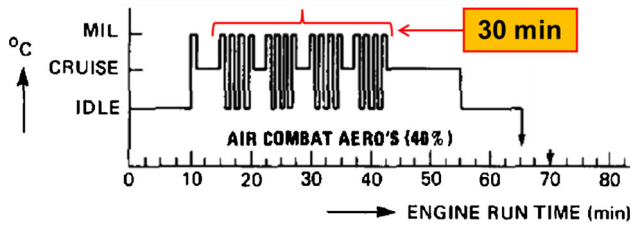

Fig. 1 Air combat aero mission profile as simulated in a burner rig (Ref 7). The *Y*-axis represents temperature (°C) and flight mode

intellectual property (IP) of the NRC, and therefore, it cannot be disclosed in this publication. The R_a values ($n = 10$) of the CoNiCrAlY BC and YSZ top coat were 5.4 ± 0.6 and 3.7 ± 0.6 μm, respectively. The CoNiCrAlY BC and YSZ top coat thicknesses of all TBCs were produced to be in the range of 200-250 and 350-400 μm, respectively.

2.2 Microstructural Characterization

In order to better preserve their real microstructures, the TBC samples were vacuum impregnated in epoxy resin prior to producing samples for characterization. These mounted samples were then cut to produce cross sections, which were re-mounted in epoxy and then ground/polished according to standard metallography procedures for TBCs. The cross-sectional microstructural features of the as-sprayed and mission-simulated TBCs were analyzed by scanning electron microscopy (SEM) coupled with an energy dispersive x-ray (EDX) chemical analysis device (S4700, Hitachi Ltd., Tokyo, Japan). The SEM pictures were taken in back-scattered mode. For the as-sprayed and mission-simulated TBCs, the EDX chemical analysis was performed on the CoNiCrAlY BC on 5 random zones at an SEM magnification of ×500, which corresponded to a probed area of ~250 μm × 180 μm. Therefore, it is important to highlight that the EDX chemical results represent a relatively broad area of the coating, and not a single detailed point. Each EDX data acquisition was performed during a 60-s probing time.

X-ray diffraction (XRD) (D8 Discovery, Brucker AXS Inc., Madison, WI, USA), using CrKα radiation in Bragg-Brentano configuration, was employed to evaluate the phase compositions of the YSZ powder and as-sprayed and mission-simulated YSZ top coat. The XRD 2θ values ranged from 40° to 130° (scanning step size of 0.05° and step time of 2.5 s).

2.3 Thermal Diffusivity and Conductivity Values

Thermal diffusivity (TD or α) and thermal conductivity (TC or κ) measurements were performed both at room and high temperatures on free-standing YSZ coatings (as-sprayed and annealed). The free-standing coatings were produced by firstly plasma spraying ''table salt'' on low carbon steel substrates, for the subsequently spraying of YSZ. The YSZ coatings were easily detached from the substrates upon water dissolution, and dried in a furnace at 150 °C for 12 h. To produce annealed YSZ samples, as-sprayed coatings were heat treated in air at 1150, 1300, and 1400 °C for 10 h in a box furnace (heating rate 300 °C/h and natural cooling to room temperature inside the furnace). Three groups of three coatings each were annealed at these three temperatures individually, i.e., no samples were annealed more than one time. The laser-flash technique (FlashLine 5000, Anter Corp., Pittsburgh, PA, USA), based on the work developed by Parker et al. (Ref 9), was employed to measure the TD values. For TD measurements, a ~1-2-μm-thick graphite layer (Graphite Spray Paint CX-01, TA Instruments, New Castle, DE, USA) was sprayed on the YSZ samples to increase the absorption of the yttrium aluminum garnet (YAG) laser ($\lambda = 1.1$ μm) radiation energy and maximize the accuracy of the measurement by the infrared sensor. The TD measurements were performed at 1 atm (101 kPa) with constant Ar gas flow of ~0.25 lpm at different temperature intervals (typically 250 °C), from RT up to 1400 °C. A total of 2 or 3 samples per YSZ coating were used for TD measurements. For each single sample, the laser-flash equipment performed three TD measurements at each pre-programed temperature level.

The density (ρ) values of the as-sprayed and heat-treated YSZ samples were measured via the Archimedes technique: $\rho\ (\mathrm{kg/m^3}) = (m_{\mathrm{dry}}/(m_{\mathrm{wet}} - m_{\mathrm{immersed}})) \times 1000$, where m is mass in grams. A total of 2 or 3 samples per coating were used to generate the density values.

The RT and high-temperature specific heat (C_p) values of the YSZ samples were estimated based on the equation developed from the APS YSZ TBC database of Wang et al. (Ref 10), ranging from RT up to 1400 °C. The general curve-fitting equation is

$$Cp\ (\mathrm{J/kgK}) = \left(m_1 + m_2 T + m_3 T^{-0.5} + m_4 T^{-2} + m_5 T^{-3}\right) \times 1000, \quad \text{(Eq1)}$$

where $m_1 = 0.60045$, $m_2 = 4.296 \times 10^{-5}$, $m_3 = 0.22845$, $m_4 = -24201$, $m_5 = 2.3668 \times 10^{-6}$, and T is the temperature in Kelvin.

After the TD, C_p and density values were determined, the TC (κ) values were calculated by using the traditional TC equation: $\kappa\ (\mathrm{W/mK}) = \alpha\ (\mathrm{m^2/s}) \times C_p\ (\mathrm{J/kg\ K}) \times \rho\ (\mathrm{kg/m^3})$. It has to be highlighted that the density values of the as-sprayed and heat-treated coatings were measured at room temperature and used to calculate the TC values reported in this work.

2.4 Thermal Gradient Laser Rig

The NRC thermal gradient laser rig is based on a 3 kW CO_2 laser, which yields a continuous beam exhibiting a wavelength of 10.6 μm over the YSZ top coat of the TBC. A compressed air jet cools the back side of the substrate. The rig is closed-loop computer-controlled; therefore, the front and back temperatures of the samples are continuously recorded during the tests. The overall schematic of the rig is shown in Fig. 2.

The temperature of the YSZ top coat was measured using a 1-color 7.9 μm wavelength D/100 (500-1800 °C) infrared pyrometer (Modline 7, Ircon Inc., Santa Cruz, CA, USA) with a spot size of ~6 mm, centered in the middle of the sample. For the substrate back side, a 1-color 5.1 μm wavelength D/100 (300-1600 °C) infrared pyrometer (IN-140/5-H, LumaSense Technologies, Santa Clara, CA, USA) was employed and also had a spot size of ~6 mm, centered in the middle of the sample. An infrared (IR) camera with a 384 × 288 pixel micro-bolometer detector at 7.5-14 μm spectral range (IR-TCM 384 IR, Jenoptik AG, Jena, Germany) coupled with a CO_2 notch filter at 8 μm was also employed to measure the overall

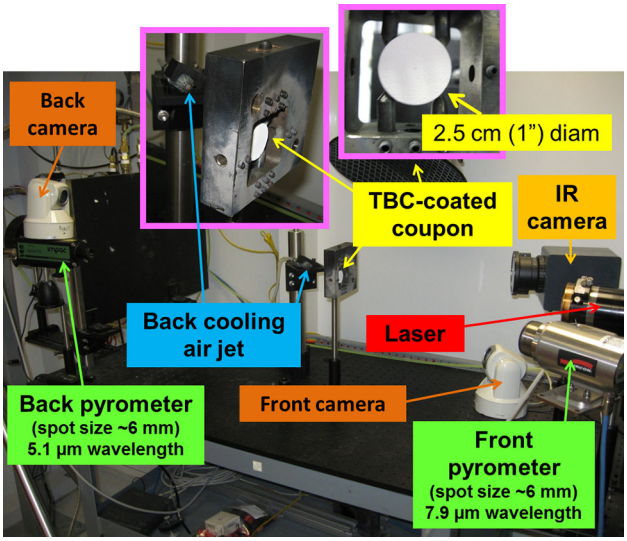

Fig. 2 Thermal gradient laser rig of the NRC

distribution of temperature on the surface of the YSZ top coat. The IR camera is used to guarantee a uniform laser beam and temperature over the surface of the TBC. In addition, two digital cameras record the images of the front and back sides of the samples during testing. The emissivity values for the YSZ top coat and oxidized Inconel 625 were measured and found to be 0.96 and 0.90, respectively.

Due to its closed-loop computer control, the laser rig can be operated in constant temperature or constant power/cooling modes. In constant temperature mode, the temperature of the YSZ top coat (T_{front}) and substrate back side (T_{back}) are kept constant during the operation. This steady state is achieved because the laser power and substrate back cooling (compressed air jet) automatically adjust their intensity levels to maintain T_{front} and T_{back} constant, thereby leading to a ΔT constant across the TBC system. It is important to highlight that the high-temperature environment, in addition to the heating and cooling cycles, will introduce important changes in the TBC microstructure (e.g., sintering, TGO growth, overall BC oxidation, and micro- and macro-cracking), which will result in overall changes of the thermal conductivity levels of the TBC. Therefore, in order to maintain T_{front} and T_{back} constant in time, laser and cooling power levels need to be adjusted. In constant power/cooling mode, as it states, the laser power and the substrate back cooling levels are kept constant during the rig operation. Therefore, in this case, the temperature of the YSZ top coat (T_{front}) and substrate back side (T_{back}) changes with time due to the microstructural changes that will occur in the TBC microstructure and thermal conductivity values.

2.5 Flight Simulation in the Thermal Gradient Laser Rig

As previously stated, the air combat aero profile mission, shown in Fig. 1, based on the burner rig simulation of Mom and Hersbach (Ref 7), was the fundamental information for the simulation performed in the laser rig, in addition to complementary data found in the open internet literature, e.g., (Ref 8). In order to perform the simulation in the laser rig, the following approach was taken. A TBC sample was placed in the rig (Fig. 2) for an initial calibration. The substrate back cooling (air jet) level was set at its maximum output. The laser power was turned on and slowly increased (manually) up to the moment when the YSZ top coat surface temperature reached a value of ~1100 °C. This YSZ surface temperature value was chosen as reference because it typically represents the maximum temperature of operation of the Inconel 625. At this temperature level, the 0.2% yield strength value of the Inconel 625 is ~10% that of RT (Ref 11). Therefore, this laser power was set to be the military (MIL) power, representing the moment when the engine is operating at 100% of its power. For the CRUISE and IDLE stages of the turbine, the estimated power values were 75 and 25% of the maximum MIL power. The summary of the flight simulation performed in the rig is found in Table 1. The graph of the profile of the laser power and substrate back cooling levels versus simulation time is shown in Fig. 3.

The overall total simulated missions (i.e., flights) lasted for 2.5 h (150 min). A total of 50 missions were simulated using the same profile shown in Table 1 and Fig. 3, totaling 125 h of testing. After 50 missions, the TBC was taken from the rig for microstructural evaluation. It is important to highlight the fact that only the laser power changed levels during the simulation. The intensity of the back side cooling (compressed air jet) was set at its maximum output and kept constant during the simulated mission. It is interesting to compare the similarities of the mission designed by Mom and Hersbach (Fig. 1) (Ref 7) and that proposed in this work (Fig. 3).

2.6 Isothermal Treatments

Isothermal treatments were employed in order to better understand to overall TBC behavior in high temperature. One as-sprayed TBC was heat treated in a furnace in air during 25 h non-stop at 1000 °C to induce BC oxidation, whereas another as-sprayed TBC was heat treated in a furnace in hydrogen (H_2) environment during 25 h non-stop at 1000 °C to avoid BC oxidation.

3. Results and Discussion

3.1 Thermal Properties

The TD and TC values for the as-sprayed and annealed APS YSZ TBCs are found in Fig. 4. The TD of the annealed samples measured in the temperature range of 1000-1400 °C exhibited an average value of ~2.6 × 10^{-7} m^2/s (Fig. 4a). The average TC value from RT up to 1400 °C of the annealed samples was ~0.85 W/mK (Fig. 4b). These values put this APS YSZ TBC within the lowest ranges of TD and TC values reported for APS YSZ TBCs in the same temperature range, as shown by Wang et al. (Ref 10).

Table 1 Steps, stages, and estimations of the flight simulation performed in the laser rig

Stage	Power, %	Time, min	Estimation
Idle/Taxi (IDLE)	25	5	Turn-on engine and taxi to runway
Take-off and climb (MIL)	100	3	Reach 13,000 feet (4 km) altitude
Cruise to combat zone (CRUISE)	75	52	Combat radius of ~1000 km and cruise speed of ~950 km/h
Air-to-air combat (MIL-IDLE-CRUISE)	100-25-75	30	50 s intervals alternating MIL and IDLE power—2.5 min intervals of CRUISE power—Fig. 1 (Ref 7)
Cruise back to base	75	55	Combat radius of ~1000 km and cruise speed of ~950 km/h
Idle/taxi (CRUISE)	25	5	Taxi to hangar and turn-off engine

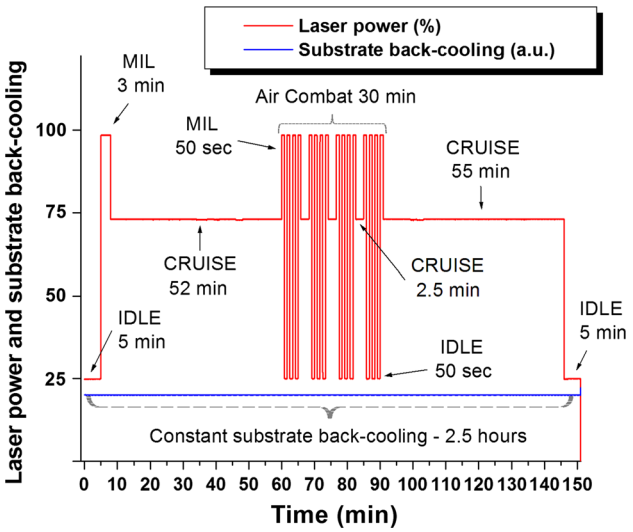

Fig. 3 Laser power level and substrate back cooling profiles and occurrence frequency in the simulated mission

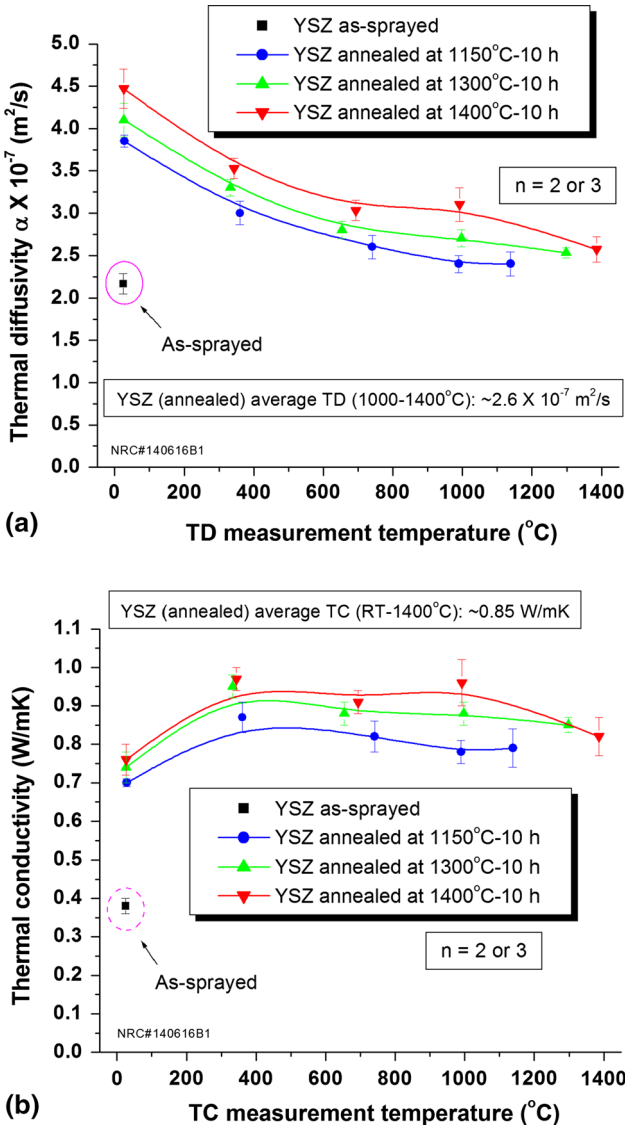

Fig. 4 (a) TD and (b) TC values for as-sprayed and annealed APS YSZ TBCs employed in this study

3.2 Simulated Flight Missions: Microstructural Behavior

A total of 50 missions were simulated in the laser rig (using the conditions depicted in Table 1 and Fig. 3) with one single TBC sample. As each simulated mission lasted for 2.5 h, the total time of testing of the TBC was 125 h. The front-view and cross-sectional pictures of an as-sprayed TBC and the TBC after 50 simulated missions are shown in Fig. 5. It is possible to notice that no major defects are observed on the TBC surface after 50 simulated missions. By looking at the cross section, no major cracking, debonding, or delaminations were observed after 50 simulated missions. The overall TBC does not show signs of cohesion or adhesion problems. In addition, no major thermally grown oxide (TGO) is observed at the YSZ/BC interface. SEM observations of other high-magnification images (not shown) supported these claims.

An EDX chemical analysis of the CoNiCrAlY BCs is reported in Table 2. The 2nd column corresponds to the nominal composition of the powder provided by its manufacturer (Ref 12). It is possible to notice the similarities between the nominal feedstock powder composition and that of the as-sprayed BC. In addition, the low oxidation state of the as-sprayed BC (<1 wt.%) showed that under ''controlled spray conditions,'' CoNiCrAlY BCs can be air plasma sprayed without exhibiting major coating oxidation. After 50 simulated missions, it is possible to visually observe an increase in the oxidation state in the splat

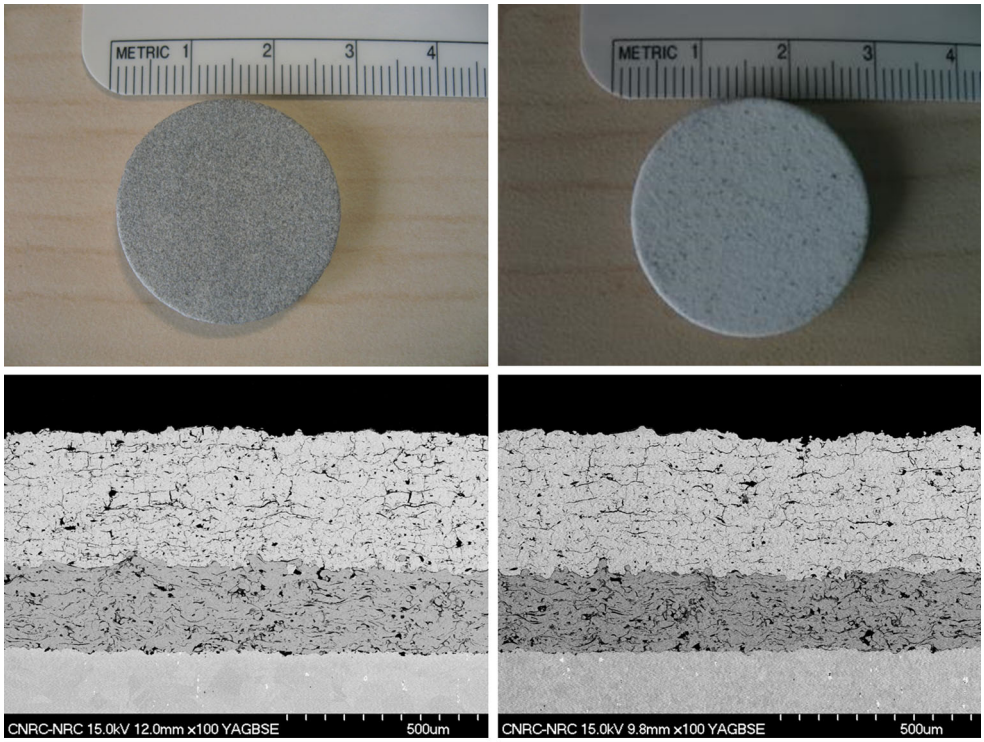

Fig. 5 Front-view and cross-sectional pictures of (a) an as-sprayed TBC and (b) TBC after 50 simulated missions

Table 2 EDX chemical analysis of the CoNiCrAlY BC of Fig. 5a and b

Element	CoNiCrAlY powder, wt.%[a]	CoNiCrAlY as-sprayed, wt.% ($n = 5$)	CoNiCrAlY 50 missions, wt.% ($n = 5$)
Co	Balance (~40)	40.1 ± 0.3	38.7 ± 1.1
Ni	29-35	35.5 ± 0.3	34.6 ± 1.1
Cr	18-24	18.5 ± 0.4	19.8 ± 0.3
Al	5-11	5.6 ± 0.2	6.5 ± 0.3
Y	0.1-0.8	Not detected	Not detected
O	n.a.	0.4 ± 0.1	0.7 ± 0.2

[a]Nominal powder composition provided by manufacturer

boundaries of the BC (Fig. 5b); nonetheless, the results of Table 2 demonstrated that it is still less than 1 wt.%, i.e., the oxidation that occurred during the mission simulation was probably not severe. The lack of a well-defined TGO (Fig. 5b) also supports this observation.

Figure 6 corroborates with this previous statement. It shows the two TBCs isothermally treated at 1000 °C during 25 h non-stop. The TBC isothermally treated in a H_2 atmosphere was dubbed the ''non-oxidized'' (Fig. 6a), whereas the one isothermally treated in air was dubbed ''oxidized'' (Fig. 6b). There was a minimum TGO formation on the oxidized TBC when comparing both microstructures. In fact, the microstructure of Fig. 5(b) (×100) and 6(b) (×100) are much alike. Therefore, at 1000 °C, no major oxidation of the BC was observed.

Therefore, due to the low TC values of the YSZ top coat at high temperatures (~0.85 W/mK) (Fig. 4), in addition to its relatively high thickness (~375 μm) (Fig. 5), as well as the natural ''good'' oxidation resistance exhibited by the BC, one may consider that the drop of temperature across the YSZ top coat was significant enough to avoid a major oxidation of the BC during the 125 h of mission simulation.

The XRD spectra of the YSZ feedstock powder, as-sprayed, and 50 mission-simulated YSZ top coats can be found in Fig. 7. No major changes in the phase structure of the powder and the YSZ top coat were observed, even after 50 simulated missions.

3.3 Simulated Flight Missions: Temperature Profiles

The profiles of the surface temperatures of the YSZ top coat and Inconel 625 substrate back side are found in

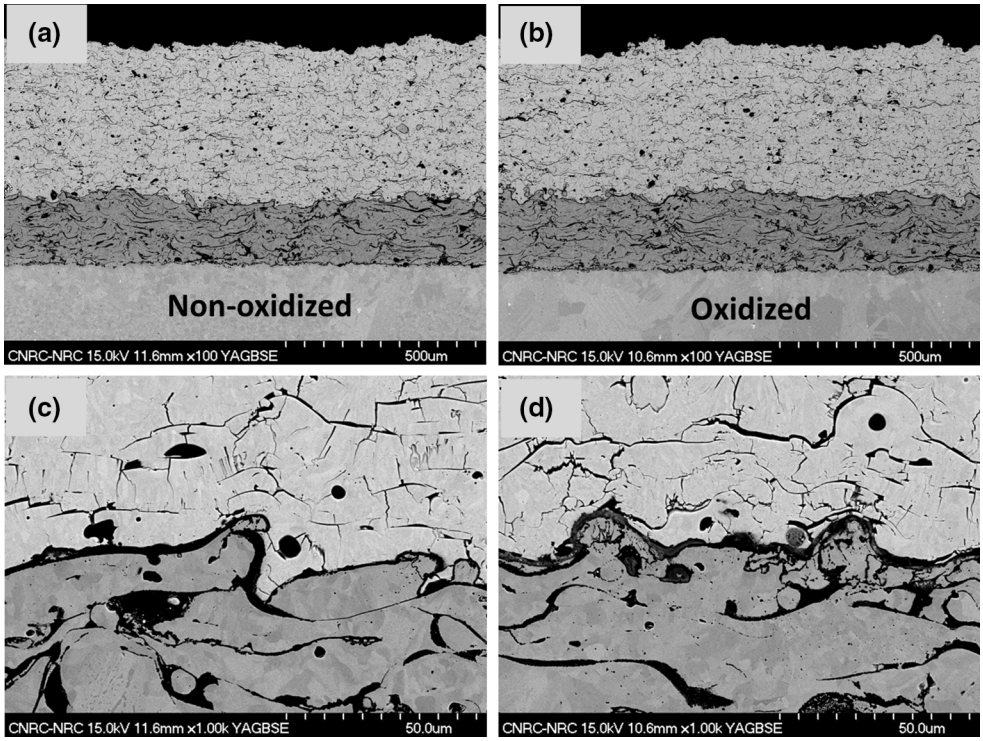

Fig. 6 Cross-sectional pictures of TBCs isothermally treated at 1000 °C during 25 h non-stop (a and c) in H_2 atmosphere (non-oxidized) and (b and d) in air (oxidized)

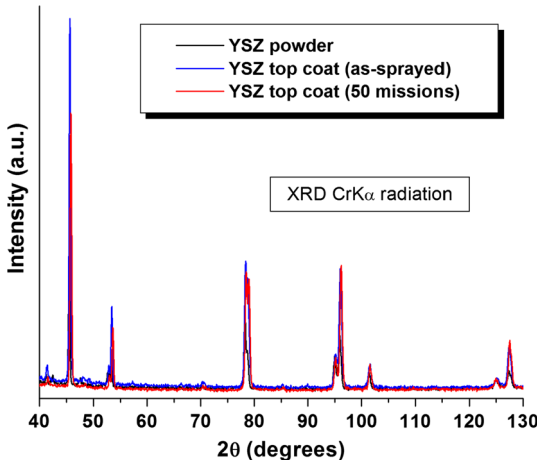

Fig. 7 XRD spectra of the YSZ powder, as-sprayed, and 50 mission-simulated YSZ top coats. The XRD intensity is given in arbitrary units (a.u.)

Fig. 8. It corresponds to the profiles of the 1st and last (50th) simulated missions. It is possible to observe that the attempt to simulate the air combat mission proposed by Mom and Hersback (Fig. 1) (Ref 7) was successful. Therefore, it is possible to simulate flight missions in the thermal gradient laser rig, as long as the profile of the flight mission is previously known or estimated, like data provided in Table 1 and profiled in Fig. 3. The overall YSZ top coat surface temperature distribution during the take-off stage is shown in the IR camera picture (Fig. 8). It is possible to observe that the temperature distribution is highly uniform at the center of the TBC sample. The simulation was performed under different sets of constant power and cooling conditions for each step of the mission (Fig. 3), i.e., they were not changed to keep the ΔT across the TBC constant. Therefore, the TBC aging effect was observed in the testing. The maximum surface temperatures of the YSZ top coat changed or evolved with time (Fig. 8 and 9). On average, the maximum YSZ top coat surface temperature dropped ~15%, from the 1st to the 50th simulated mission. For example, for the very 1st take-off, the maximum TBC surface temperatures (YSZ and Inconel 625) were ~1100 and ~750 °C, whereas for the 50th take-off, there were ~900 and ~700 °C.

This behavior can be partially explained based on the data of Fig. 4 and data available in the literature. Patterson and Sohn (Ref 13) measured the TC values of APS CoNiCrAlY coatings. The average TC values for an as-sprayed and air-annealed (1124 °C-300 h) APS CoNiCrAlY BC, measured in the 800-1100 °C range, were ~28 and ~25 W/mK, respectively (in spite of the BC oxidation). Here there are two competing effects. The oxidation is probably decreasing the TC values of the BC; in contrast, the sintering effects are increasing those same values. Therefore, the low ~10% TC value reduction of the annealed BC is understandable. It needs to be pointed out that the 1st take-off (Fig. 7a) occurred with an as-sprayed TBC, whereas the 50th take-off (Fig. 7b) occurred with the same TBC after 120 h of thermal exposure. Figure 4

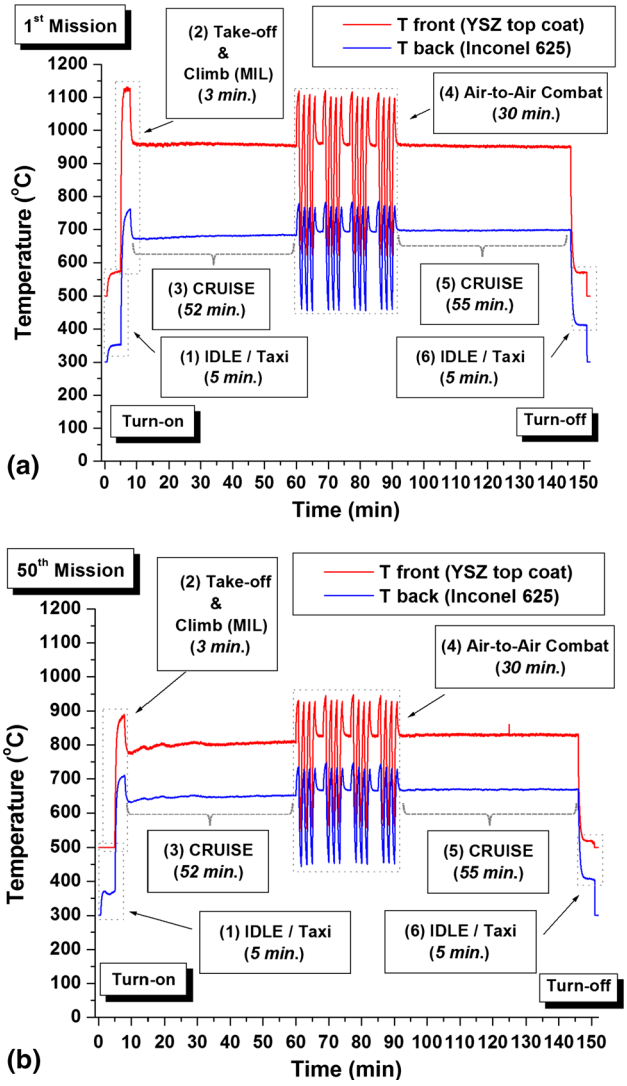

Fig. 8 TBC surface temperature profiles of the (a) 1st and (b) last (50th) flight simulated missions

shows that the as-sprayed TC value of the YSZ coating of this study increases to about 2× that of RT after annealing and when measured at high temperatures. This TC growth of ~100% was also reported by Tan et al. (Ref 14) for APS YSZ TBCs. Therefore, as the TC value of the YSZ top coat increases after the simulation begins, and that of the BC remains almost unchanged for the same conditions, one may hypothesize that the YSZ top coat surface temperature value should drop with time. This happens because the laser power and substrate back cooling levels remain unchanged for each single step of the simulation, during the 50 simulated missions. As the TC value of the YSZ top coat increases, the heat transfer to the metallic substrate also increases, thereby lowering the surface temperature of the top coat. Once again, the substrate back cooling level was kept constant at its maximum intensity during the whole stage of the simulated mission (Fig. 3).

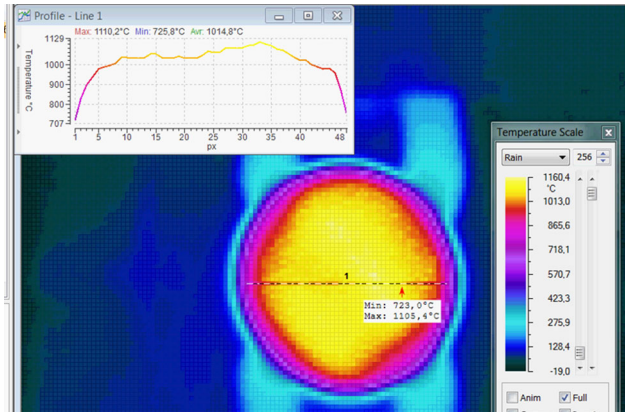

Fig. 9 IR picture of TBC surface during take-off (1st simulated mission)

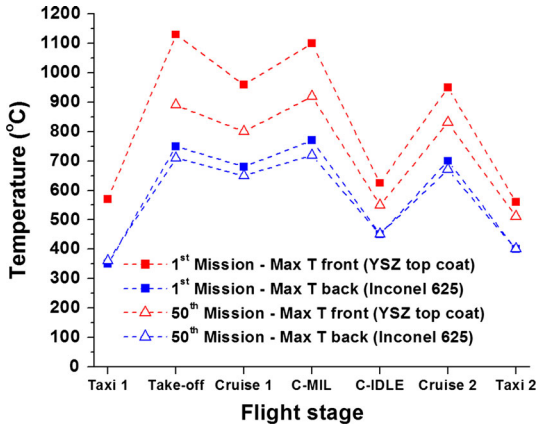

Fig. 10 Maximum TBC and back side substrate surface temperatures at the 1st and last (50th) flight simulated missions

It needs to be pointed out that during the heat treatment of the free-standing YSZ coatings in a box furnace (for further TD and TC measurements (Fig. 4)), there was no temperature gradient (ΔT) along the thicknesses of the YSZ top coats. In contrast, during the flight simulation in the laser rig, the ΔT was present (Fig. 7). Therefore, one can hypothesize that only a small thickness (next to the coating surface) of the YSZ TBC was subjected to the highest temperature levels during the flight simulations. The YSZ TBC zone adjacent to the bond coat was probably at lower temperatures, and consequently its TC values may have been closer to those of the as-sprayed ones, even after 50 simulated missions. In other words, a gradient of TD and TC values along the YSZ TBC thickness was probably generated during the flight simulation.

Surprisingly, it is noticeable that the Inconel 625 back side surface temperature levels remained relatively constant from the 1st to the 50th simulated mission (Fig. 9). Therefore, the significant lowering of the ΔT values across the TBC from the 1st to the 50th simulated mission (Fig. 10) was mainly related to the YSZ top coat. This effect may be related to the gradient of TD and TC values

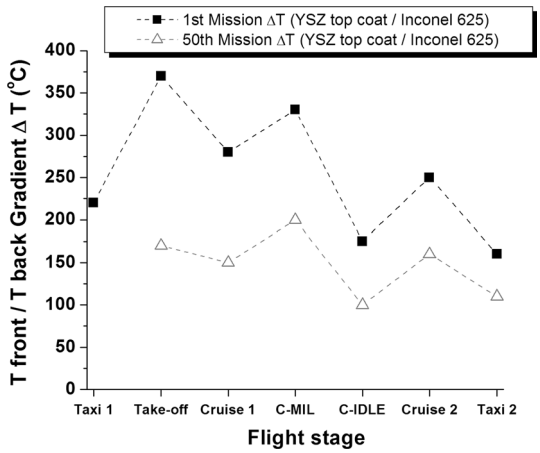

Fig. 11 Maximum TBC ΔT values at the 1st and last (50th) flight simulated missions

in the YSZ top coat, as discussed in the last paragraph. Figure 11 shows in detail the ΔT values across the TBC-substrate system in different regions of the flight, for the 1st and 50th simulated missions.

4. Conclusions

Closed-loop computer-controlled thermal gradient laser rig systems can be employed to simulate the ΔT across TBCs of different regions of a turbine engine during flight missions, including complex ones like that of a fighter jet in air-to-air combat (as long as the mission profile is known or estimated). This work showed that such studies can provide valuable information about the gradient across the TBC during different stages of the flight, as well as the heating/cooling rates with respect to their evolution in time as a response to the TBC aging. This type of test could become very important for TBC engineering and life prediction in the different components of gas turbines engines.

Acknowledgments

The authors would like to acknowledge the great contributions of the following technical officers of the NRC Boucherville site. Without them, this work could not have been done: Bernard Harvey and Mario Lamontagne for engineering the laser rig. Jean-Claude Tremblay for TBC production and laser rig operation. David Delagrave for metallography prepping and Karine Theberge for performing SEM-EDX-XRD analyses. The authors are also thankful to Prof. Frank W. Zok (University of California, Santa Barbara, CA, USA) for sharing with the NRC key sets of information regarding laser rig engineering. Finally, the authors would like to acknowledge the contribution of the NRC Chief Test Pilot (CF-18 Royal Canadian Air Force (RCAF) retired Capt. Paul ''Rose'' Kissmann) and RCAF CF-18 fighter pilots for providing feedback on the fighter mission profile.

References

1. D.J. Wortman, B.A. Nagaraj, and E.C. Duderstadt, Thermal Barrier Coatings for Gas Turbine Use, *Mater. Sci. Eng. A*, 1989, **121**, p 433-440
2. A. Feuerstein, J. Knapp, T. Taylor, A. Ashary, A. Bolcavage, and N. Hitchman, Technical and Economical Aspects of Current Thermal Barrier Coating Systems for Gas Turbine Engines by Thermal Spray and EBPVD: A Review, *J. Therm. Spray Technol.*, 2008, **17**(2), p 199-213
3. T. Patterson, A. Leon, B. Jayaraj, J. Liu, and Y.-H. Sohn, Thermal Cyclic Lifetime and Oxidation Behavior of Air Plasma Sprayed CoNiCrAlY Bond Coats for Thermal Barrier Coatings, *Surf. Coat. Technol.*, 2008, **203**, p 437-441
4. R. Vassen, F. Cernushi, G. Rizzi, A. Scrivani, N. Markocsan, L. Ostergren, A. Kloosterman, R. Mevrel, J. Feist, and J. Nicholls, Recent Activities in the Field of Thermal Barrier Coatings Including Burner Rig Testing in the European Union, *Adv. Eng. Mater.*, 2008, **10**(1), p 907-921
5. D. Zhu and R.A. Miller, Thermal Conductivity and Elastic Modulus Evolution of Thermal Barrier Coatings under High Heat Flux Conditions, *J. Therm. Spray Technol.*, 2000, **9**(2), p 175-180
6. J. Manara, M. Arduini-Schuster, H.-J. Ratzer-Scheibe, and U. Schulz, Infrared-Optical Properties and Heat Transfer Coefficients of Semitransparent Thermal Barrier Coatings, *Surf. Coat. Technol.*, 2009, **203**, p 1059-1068
7. A.J.A. Mom and J.C. Hersbach, Performance of High Temperature Coatings on F100 Turbine Blades under Simulated Service Conditions, *Mater. Sci. Eng. A*, 1987, **87**, p 361-367
8. www.saabgroup.com/en/Air/Gripen-Figher-System/. Accessed April 1st, 2014
9. W.J. Parker, R.J. Jenkins, G.L. Abbott, and C.P. Butler, Flash Method of Determining Thermal Diffusivity, Heat Capacity, and Thermal Conductivity, *J. Appl. Phys.*, 1961, **32**(9), p 1679-1684
10. www.haynesintl.com/pdf/h3073.pdf. Accessed April 1st, 2014
11. H. Wang, R.B. Dinwiddie, and W.D. Porter, Development of a Thermal Transport Database for Air Plasma Sprayed ZrO_2-Y_2O_3 Thermal Barrier Coatings, *J. Therm. Spray Technol.*, 2010, **19**(5), p 879-883
12. www.oerlikon.com/ecomaXL/files/metco_DSMTS-0092.5_CoNiCrAlY.pdf&download=1. Accessed October 12th, 2014
13. T.J. Patterson and Y.-H. Sohn, http://etd.fcla.edu/CF/CFE0002400/Patterson_Travis_J_200812_MS.pdf. Accessed October 12th, 2014
14. Y. Tan, J.P. Longtin, S. Sampath, and H. Wang, Effect of the Starting Microstructure on the Thermal Properties of As-Sprayed and Thermally Exposed Plasma-Sprayed YSZ Coatings, *J. Am. Ceram. Soc.*, 2009, **92**(3), p 710-716